

Modulating Pt---Pt Metal–Metal Interactions through Conformationally Switchable Molecular Tweezer/Guest Complexation

Xiaolong Zhang,[‡] Lei Ao,[‡] Yifei Han, Zhao Gao, and Feng Wang*

CAS Key Laboratory of Soft Matter Chemistry, iChEM (Collaborative Innovation Center of Chemistry for Energy Materials), Department of Polymer Science and Engineering, University of Science and Technology of China, Hefei, Anhui 230026, P. R. China. E-mail: drfwang@ustc.edu.cn.

Supporting Information

1.	<i>Materials and methods</i>	S2
2.	<i>Photophysical behavior of 1b</i>	S3
3.	<i>pH-Responsive conformational switch of 1b</i>	S4
4.	<i>Non-covalent complexation between 1b and 2</i>	S5
5.	<i>Non-covalent complexation between 1a and 2</i>	S7
6.	<i>Non-covalent complexation between 1b and 3</i>	S8
7.	<i>Supramolecular polymerization between 5 and 6</i>	S10
8.	<i>Synthesis of molecular tweezer 1b</i>	S12
9.	<i>Synthesis of monomers 5 and 6</i>	S17

1. Materials and methods

Iodomethane, 4-hydroxybenzaldehyde, 1-bromobutane, copper(I) iodide (CuI) were reagent grade and used as received., diphenylammonium triflate (DPAT), [Pt(tpy)Cl](BF₄), [Pt(C^N^N)Cl], [Pt(C^N^C)(DMSO)], 5-bromo-2-methoxyacetophenone, **2**, **3**, the dibenzylbromide compound were synthesized according to the previously reported procedures.^{S1-S6} Other reagents and solvents were employed as purchased.

¹H NMR spectra was collected on a Varian Unity INOVA-300 spectrometer with TMS as the internal standard. ¹³C NMR spectra were recorded on a Varian Unity INOVA-300 spectrometer at 75 MHz. Electrospray ionization mass spectra (ESI-MS) were obtained on a Bruker Esquire 3000 plus mass spectrometer (Bruker-Franzen Analytik GmbH Bremen, Germany), equipped with an ESI interface and ion trap analyzer. UV/Vis spectra were recorded on a UV-1800 Shimadzu spectrometer. Fluorescent spectra were recorded on a Fluoromax-4 spectrofluorometer. Titration Calorimetry (ITC) experiments were carried out with a Microcal VP-ITC apparatus at 298 K.

Computational details: The optimized structures were optimized by using G09 D.01 software packages.^{S7} The Pt atoms were described by the Lanl2dz core potential. Considering that the computation of complex **1b/2** is time-consuming, the basis sets for the non-metallic elements are decreased to 3-21G.

General method for the determination of heterodimeric binding constants via UV-Vis titration experiments: The measurement depends on the UV/Vis intensity changes of MMLCT absorption band upon UV-Vis titration. Briefly, treating the collected absorbance data (*A*) vs concentration of the titrating species (*C_A*) with a non-linear least-squares curve-fitting equation affords the binding constants. For 1 : 1 host/guest complexation, the binding constant is calculated according to the following equation:

$$A = A_0 + \frac{A_{\text{lim}} - A_0}{2C_0} \left[C_0 + C_A + 1/K_S - \left[(C_0 + C_A + 1/K_S)^2 - 4C_0C_A \right]^{1/2} \right] \quad (\text{Eq. S1})$$

In particular, *A*₀ and *A* are the absorbance intensity of the titrated sample at the MMLCT band with and without presence of the titrating species, respectively. [*C*₀] is the total concentration of the titrated sample, while [*C*_A] is the concentration of the titrating species. *A*_{lim} is the limiting value of absorbance in the presence of excess donor and *K*_S is the binding constant.

2. Photophysical behavior of **1b**

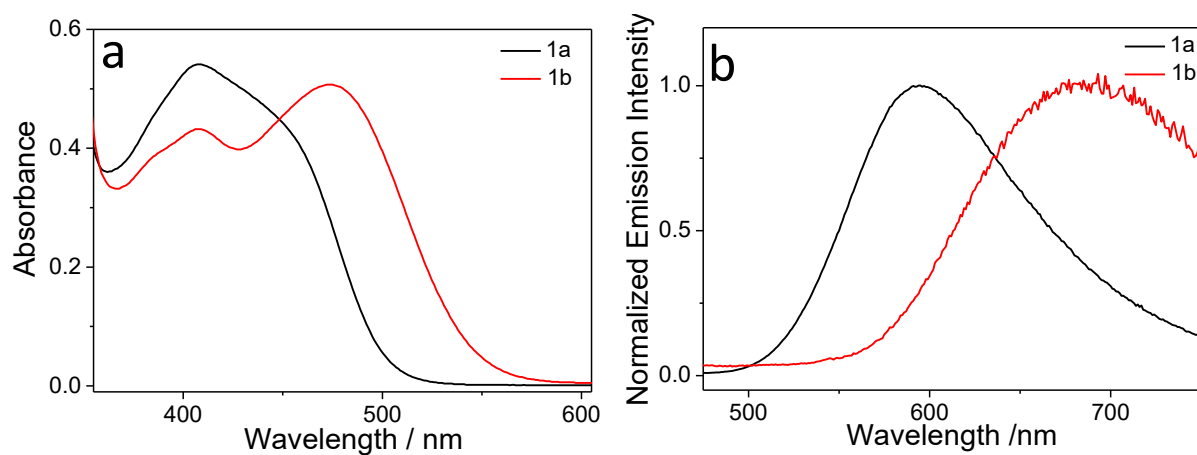


Figure S1. a) UV/Vis and b) fluorescent spectra (CHCl₃/MeOH = 1 : 1, v/v, 0.05 mM) of molecular tweezers **1a** (black line) and **1b** (red line). As can be seen, the LLCT absorption band of **1b** ($\lambda_{\text{max}} = 475$ nm) is red-shifted than that of **1a** ($\lambda_{\text{max}} = 440$ nm). Moreover, the fluorescent experiments also validate bathochromic-shifted MLCT/LLCT emission signal of **1b** ($\lambda_{\text{max}} = 685$ nm) than that of **1a** ($\lambda_{\text{max}} = 595$ nm).

3. pH-Responsive conformational switch of **1b**

As we know, **1b** is capable of undergoing mechanical transition from “U”- to “W”-shaped conformation upon addition of acid. To evaluate the role of two methoxy groups in response to pH variation, **4a–b** (Figure 1) were initially served as the model compounds. The ^1H NMR signals of **4a–b** and **1b** were monitored by adding equimolar amount of TFA into the corresponding $\text{CDCl}_3/\text{CD}_3\text{OD}$ (1 : 1, v/v) solution. The ^1H NMR spectra are shown in Figure 1 in the main text. The quantitative chemical shift changes are listed in Table S1.

Table S1. Chemical shift changes of **4a–b** and **1b** upon addition of TFA.

Hx	4a			4b			1b		
	neutral state	acidic state	$\Delta\delta$	neutral state	acidic state	$\Delta\delta$	neutral state	acidic state	$\Delta\delta$
H ₁	/	/	/	/	/	/	9.24	9.22	-0.02
H ₂	/	/	/	/	/	/	7.77	7.81	+0.04
H ₃	/	/	/	/	/	/	8.52	8.58	+0.06
H ₄	/	/	/	/	/	/	8.57	8.63	+0.06
H ₅	8.27	8.15	-0.12	7.88	7.79	-0.09	7.96	7.88	-0.08
H ₆	7.58	7.71	+0.13	7.53	7.77	+0.24	7.59	7.84	+0.25
H ₇	7.50	7.59	+0.09	7.04	7.23	+0.19	7.10	7.27	+0.17
H ₈	8.17	8.04	-0.13	3.92	4.03	+0.11	3.97	4.09	+0.12
H ₉	7.91	8.10	+0.19	7.86	8.19	+0.33	7.92	8.24	+0.32
H ₁₀	7.75	7.90	+0.15	7.67	7.95	+0.27	7.73	7.99	+0.26
H ₁₁	7.07	7.12	+0.05	7.04	7.16	+0.12	7.07	7.17	+0.10

Note: the chemical shift changes of H₆, H₉, H₁₀ were marked in color.

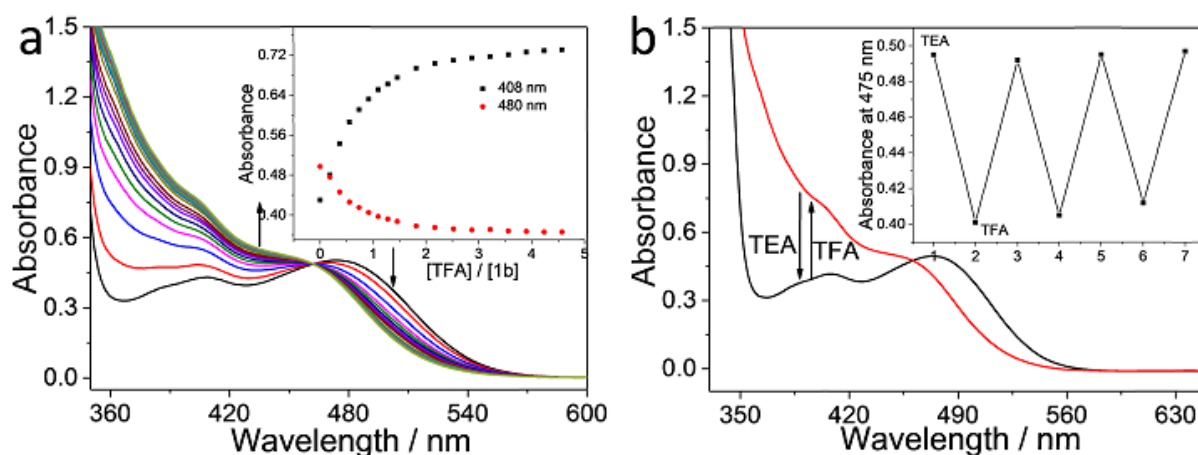


Figure S2. a) UV-Vis absorbance changes upon gradual addition of TFA into **1b** ($\text{CHCl}_3/\text{MeOH} = 1 : 1$, v/v , 0.05 mM). As can be seen, an isosbestic point appears at 462 nm. Inset: intensity changes of UV-Vis absorbance at 480 and 408 nm versus $[\text{TFA}]/[\mathbf{1b}]$. b) UV-Vis absorbance changes of **1b** ($\text{CHCl}_3/\text{MeOH} = 1:1$, v/v) upon the successive addition of TFA and TEA. Inset: the absorbance intensity at 475 nm for multiple TFA/TEA cycles.

4. Non-covalent complexation between **1b** and **2**

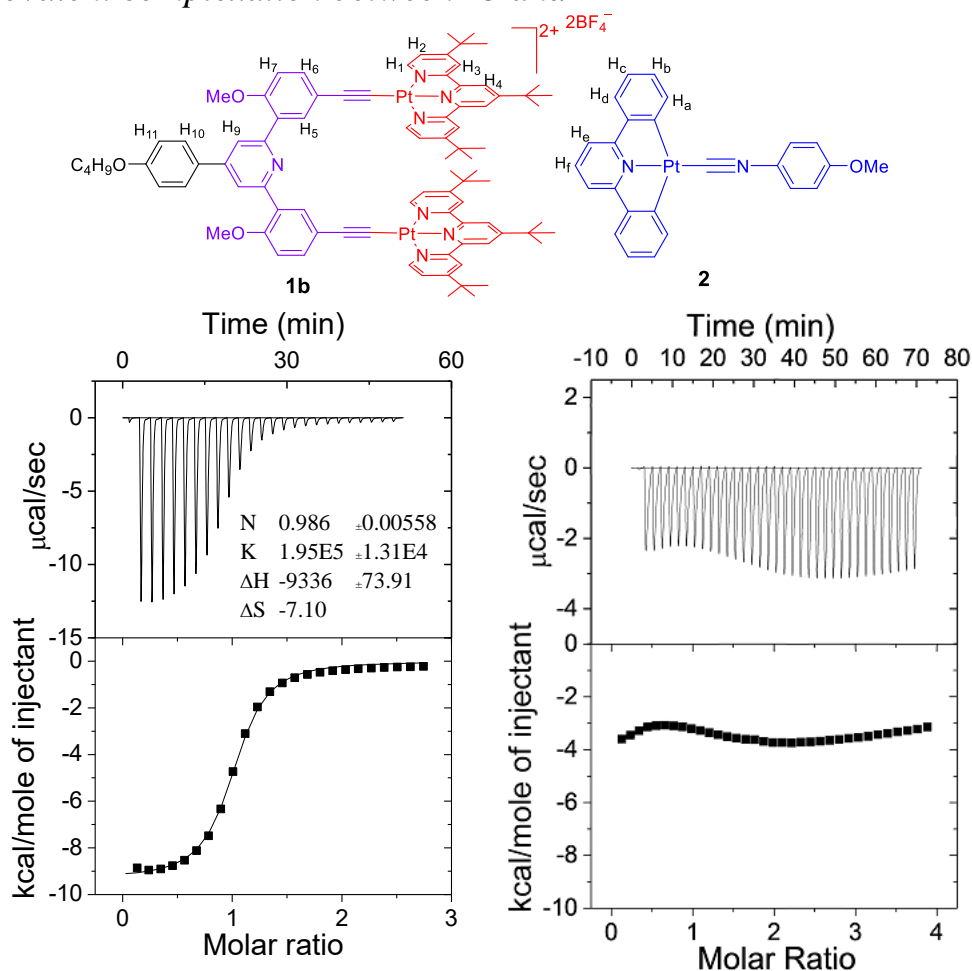


Figure S3. ITC data performed by consecutive injecting of **2** (4.00 mM) into the CHCl₃/MeOH (1 : 1 v/v) solution of a) **1b** (0.20 mM); b) the mixture of **1b** (0.20 mM) and TFA (1.60 mM, CHCl₃/MeOH = 1 : 1, v/v). As can be seen, negligible ITC heat exchange occurs when titrating **2** into the mixture solution of **1b** and TFA. Such phenomena suggest that **1b** undergoes “U”- to “W”-shaped conformational transition upon adding the acid, which influences non-covalent binding capability toward the complementary guest **2**. The result is in stark contrast to that at the neutral state.

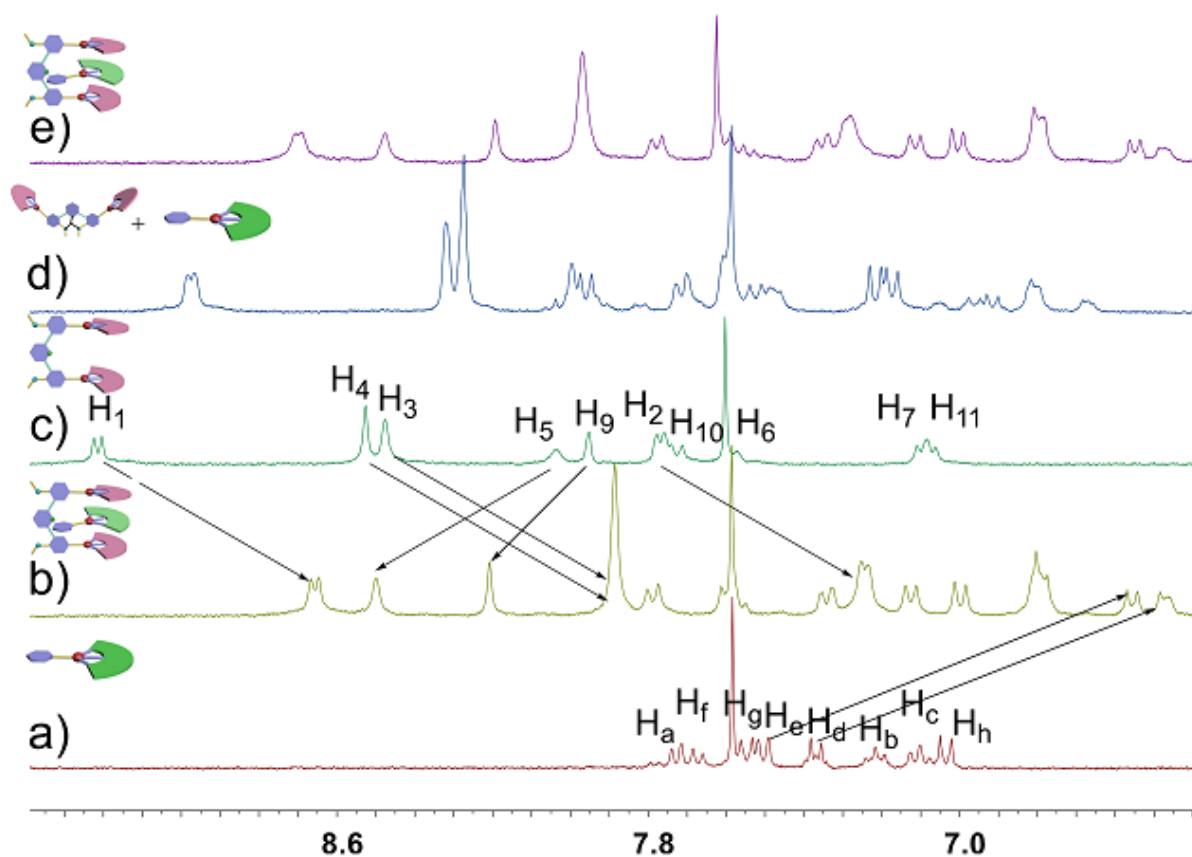


Figure S4. Partial ^1H NMR spectra (300 MHz, $\text{CDCl}_3 : \text{CD}_3\text{OD} = 1 : 1$, v/v, 6.00 mM for each monomer) of a) **2**; b) **1b/2**; c) **1b**; d) the mixture of **1b/2** and excessive amount of TFA; e) the successive addition of triethylamine to the mixture of **1b/2** and excessive amount of TFA.

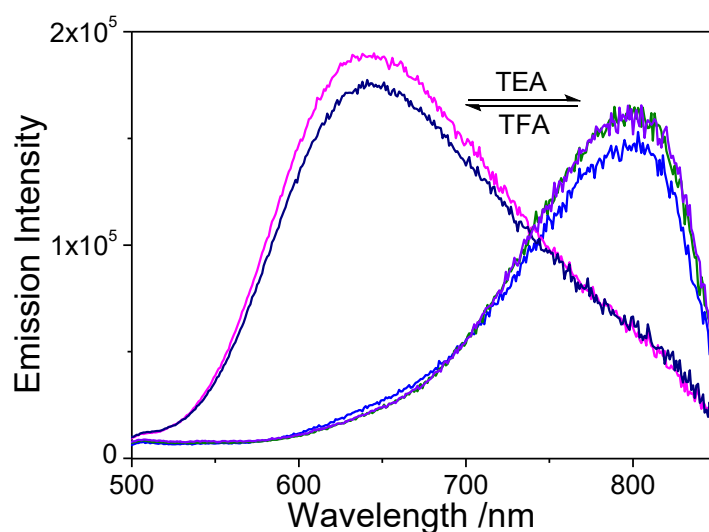


Figure S5. Fluorescent spectral changes upon successive addition of TFA and TEA into **1b/2**. As can be seen, the MMLCT emission band disappears upon adding excessive amount of TFA into **1b/2**. The vanishing of Pt(II)---Pt(II) metal–metal interactions provide direct evidence for the release of **2** from the cavity of **1b**. Simultaneously, a new emission band ($\lambda_{\text{max}} = 645 \text{ nm}$) emerges, which exactly correlate to the MLCT/LLCT spectroscopic bands of **1b** at the protonated state.

5. Non-covalent complexation between **1a** and **2**

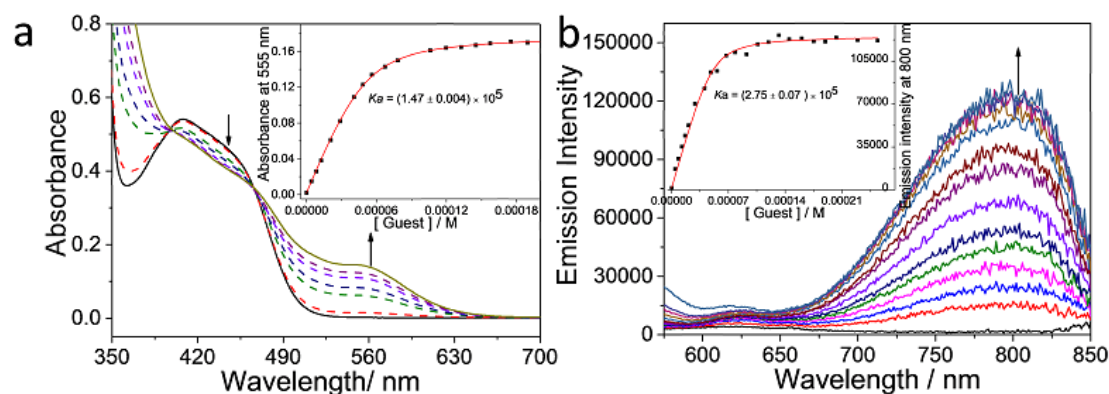


Figure S6. a) UV-Vis absorbance changes upon gradual addition of **2** into **1a** ($\text{CHCl}_3/\text{MeOH} = 1 : 1$, v/v , 0.05 mM). Inset: intensity changes of UV-Vis absorbance at 555 nm and non-linear curve fitting (red line). b) Fluorescent changes upon gradual addition of **2** in **1a** ($\text{CHCl}_3/\text{MeOH} = 1 : 1$, v/v , 0.05 mM). Inset: intensity changes of emission intensity at 800 nm and non-linear curve fitting (red line).

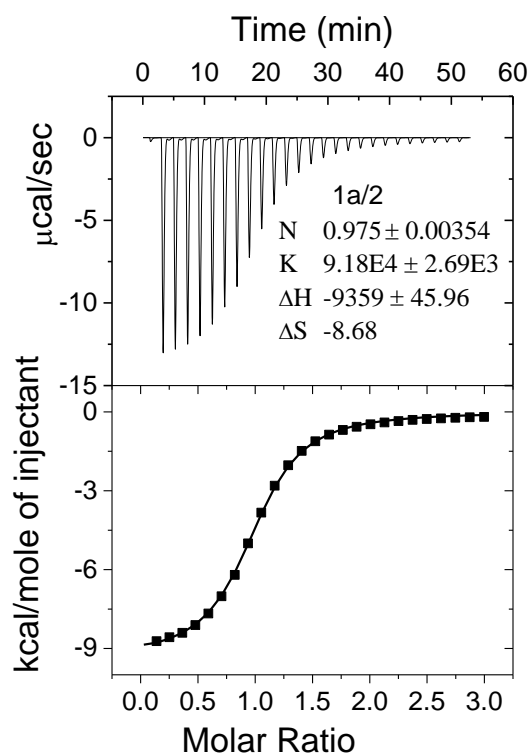


Figure S7. ITC data performed by consecutive injecting of **2** (4.00 mM) into the $\text{CHCl}_3/\text{MeOH}$ (1 : 1 v/v) solution of **1a** (0.20 mM). The binding stoichiometry between **1a** and **2** is determined to be 1 : 1, as manifested by the abrupt change in the titration curve. Fitting the exothermic isotherm data with a one-site model provides the K_a value of $(9.18 \pm 0.27) \times 10^4 \text{ M}^{-1}$ for the **1a/2** complex.

6. Non-covalent complexation between **1b** and **3**

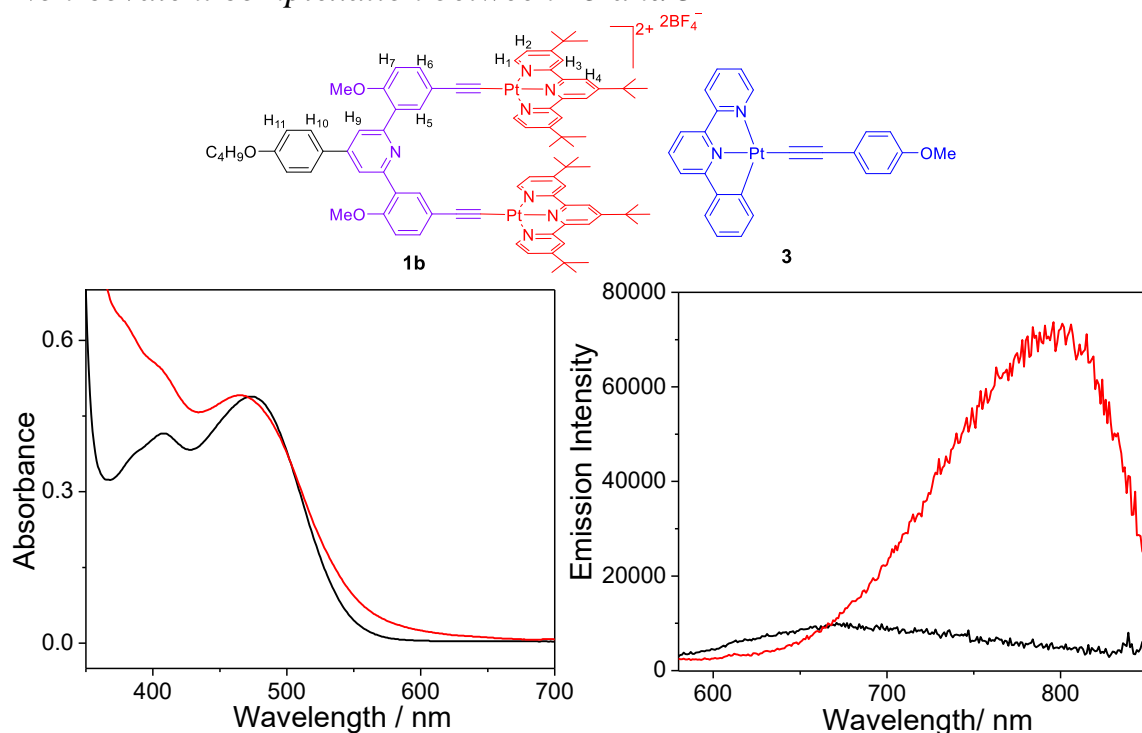


Figure S8. a) UV-Vis absorbance and b) fluorescent changes upon adding equimolar amount of **3** into **1b** (CHCl₃/MeOH = 1 : 1 v/v, 0.05 mM). Complex **1b/3** also shows the presence of bathochromic-shifted absorbance and emission bands, despite that their intensities are a little lower than those of **1b/2**.

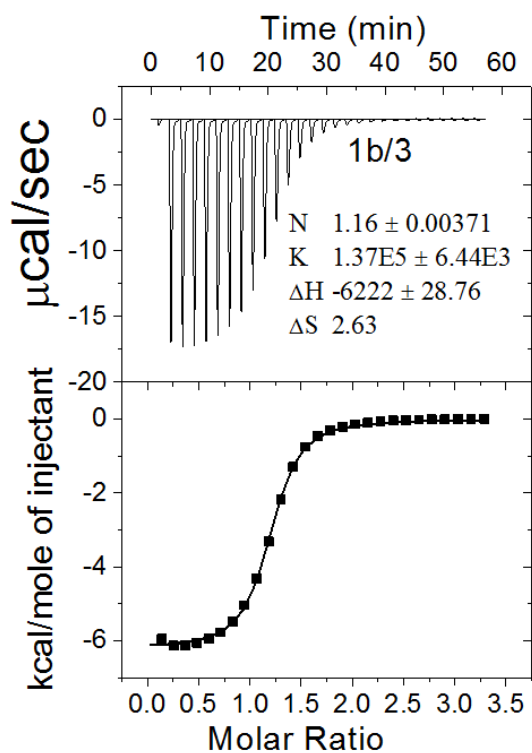


Figure S9. ITC data performed by consecutive injecting of **3** (4.00 mM) into the CHCl₃/MeOH (1 : 1 v/v) solution of **1b** (0.20 mM). The binding stoichiometry between **1b** and **3** is determined to be 1 : 1, as manifested by the abrupt change in the titration curve. Fitting the exothermic isotherm data with a one-site model provides the K_a value of $(1.37 \pm 0.06) \times 10^5 \text{ M}^{-1}$ for the **1b/3** complex.

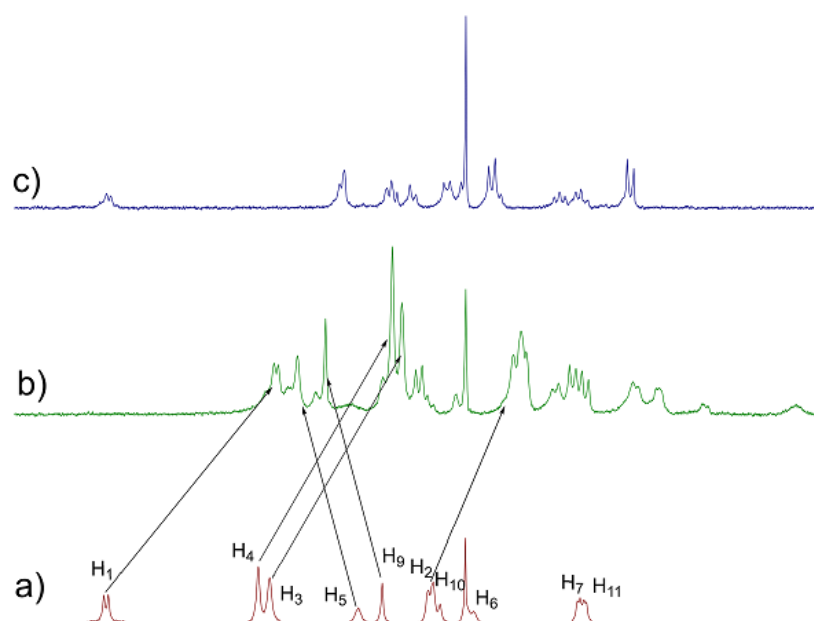


Figure S10. Partial ^1H NMR spectra (300 MHz, $\text{CDCl}_3 : \text{CD}_3\text{OD} = 1 : 1$, v/v, 6.00 mM for each monomer) of a) **3**; b) **1b/3**; c) **1b**.

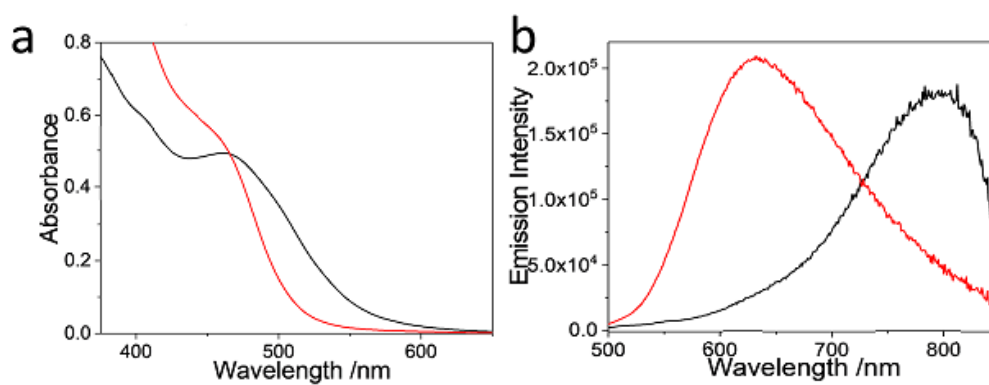


Figure S11. a) UV-Vis absorbance and b) fluorescent changes of a 1 : 1 mixture of **1b** and **3** in $\text{CHCl}_3/\text{MeOH}$ (1 : 1, v/v, 0.05 mM) before (black lines) and after (red lines) adding TFA.

7. Supramolecular polymerization between **5** and **6**

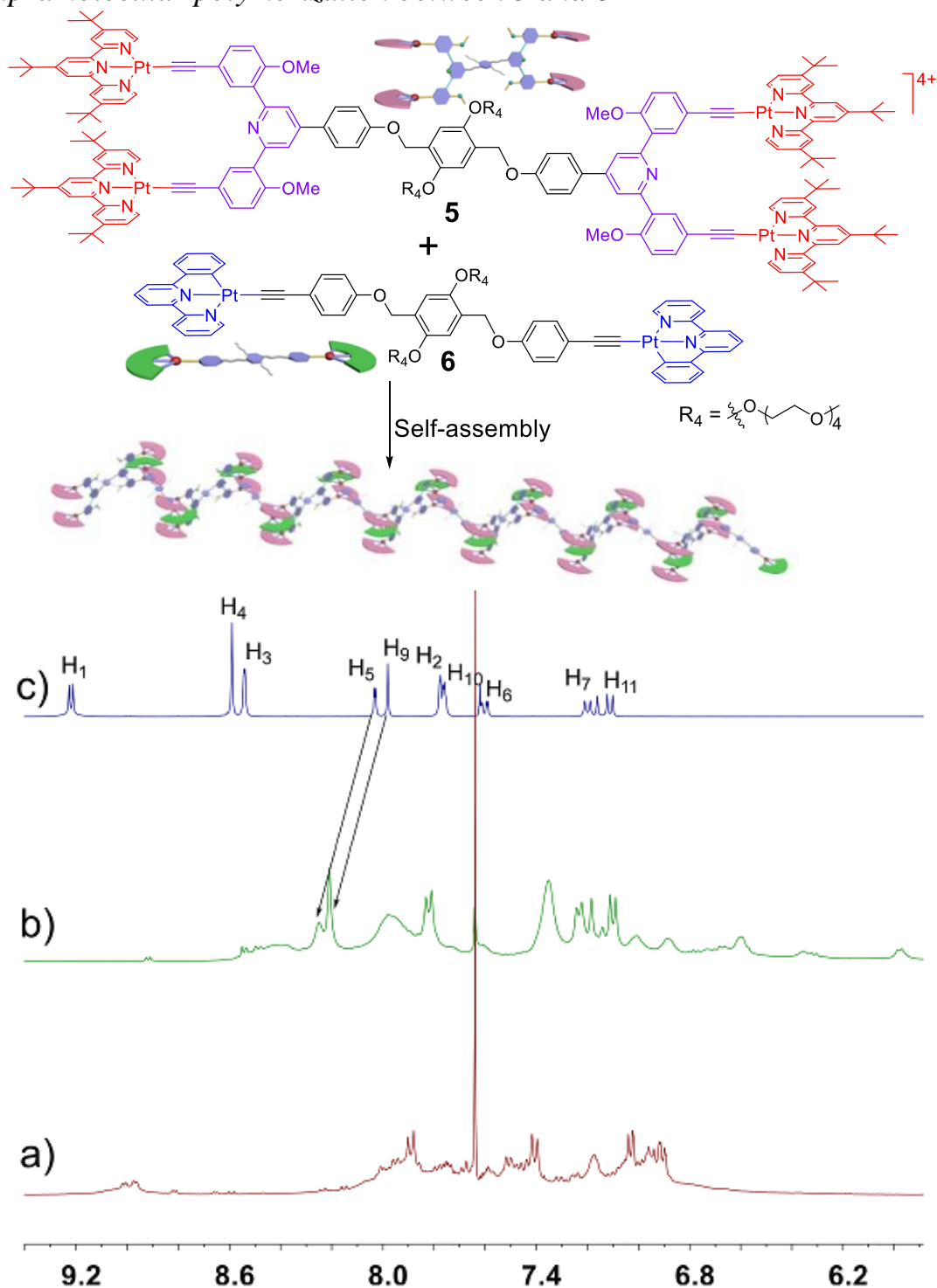


Figure S12. Partial ^1H NMR spectra (300 MHz, $\text{CDCl}_3 : \text{CD}_3\text{OD} = 1 : 1, v/v, 10.0 \text{ mM}$ for each monomer) of a) **6**; b) **5/6**; c) **5**. The chemical shift tendencies are highly consistent with those of complex **1b/3** (Fig. S10). Moreover, the ^1H NMR aromatic resonances for complex **5/6** become broad, suggesting the formation of large-sized supramolecular assemblies due to the multivalent molecular tweezer/guest complexation.

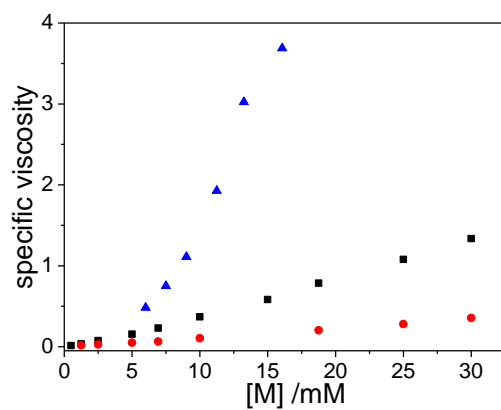


Figure S13. Specific viscosities of **5** (■), **6** (●), and complex **5/6** (▲) versus monomer concentration in CH₂Cl₂/MeOH (5 : 1, v/v).

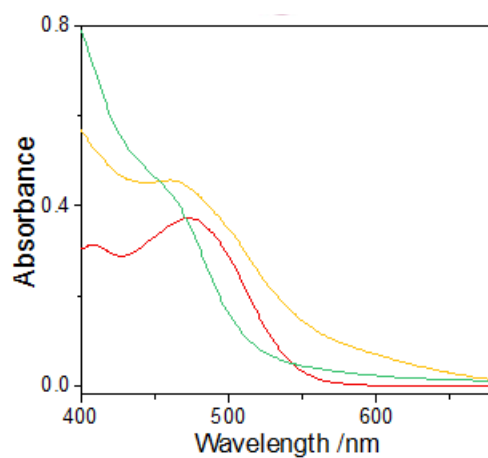
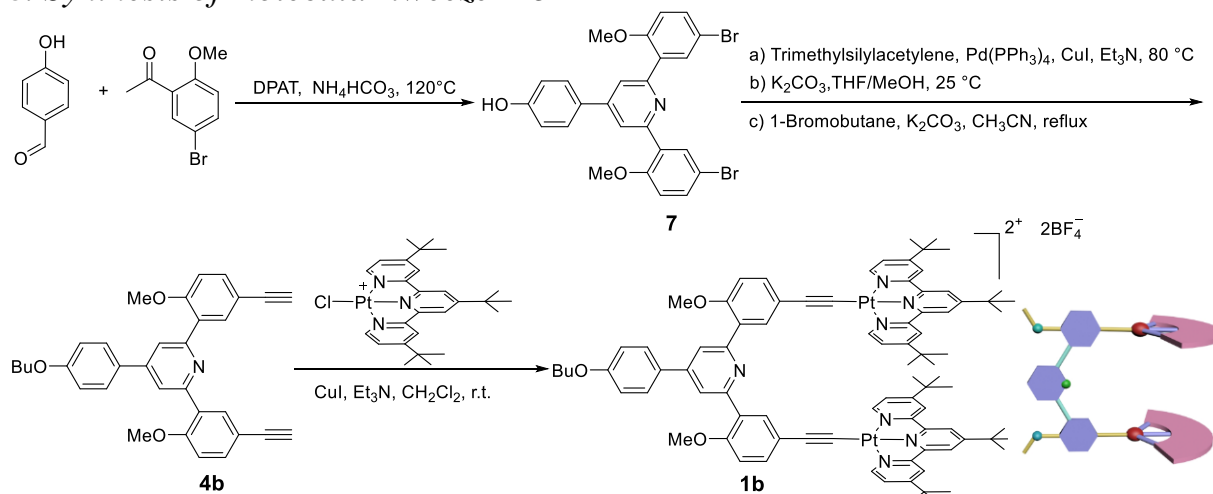


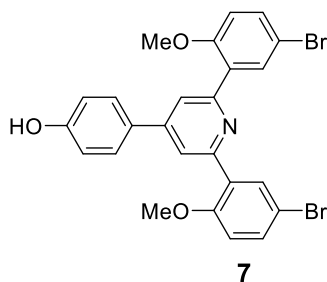
Figure S14. UV-Vis spectra of **5** (red line), complex **5/6** before (yellow line) and after (green line) adding excessive amount of TFA.

8. Synthesis of molecular tweezer **1b**



Scheme S1. Synthetic route to molecular tweezer **1b**.

7.1. Synthesis of **7**



DPAT (215 mg, 0.67 mmol) was added to a mixture of 5-bromo-2-methoxyacetophenone (4.82 g, 21.0 mmol), 4-hydroxybenzaldehyde (1.03 g, 8.41 mmol), and NH₄HCO₃ (3.33 g, 42.1 mmol). The mixture was stirred at 120 °C for 36 hours. After the reaction was complete, the solvent was evaporated under reduced pressure, and the residue was extracted with H₂O/CH₂Cl₂. The combined organic extracts were dried over anhydrous Na₂SO₄ and evaporated with a rotary evaporator. The residue was purified by flash column chromatography (petroleum ether/CH₂Cl₂, 1 : 1, v/v as the eluent) to afford **7** as a light yellow solid (1.49 g, 33%). ¹H NMR (300 MHz, CDCl₃, 298 K) δ (ppm): 7.89 (d, *J* = 2.6 Hz, 2H), 7.84 (s, 2H), 7.52–7.46 (m, 2H), 7.39 (d, *J* = 4.9 Hz, 2H), 6.96 (d, *J* = 9.0 Hz, 2H), 6.90 (d, *J* = 6 Hz, 2H), 5.20 (s, 1H), 3.82 (s, 6H).

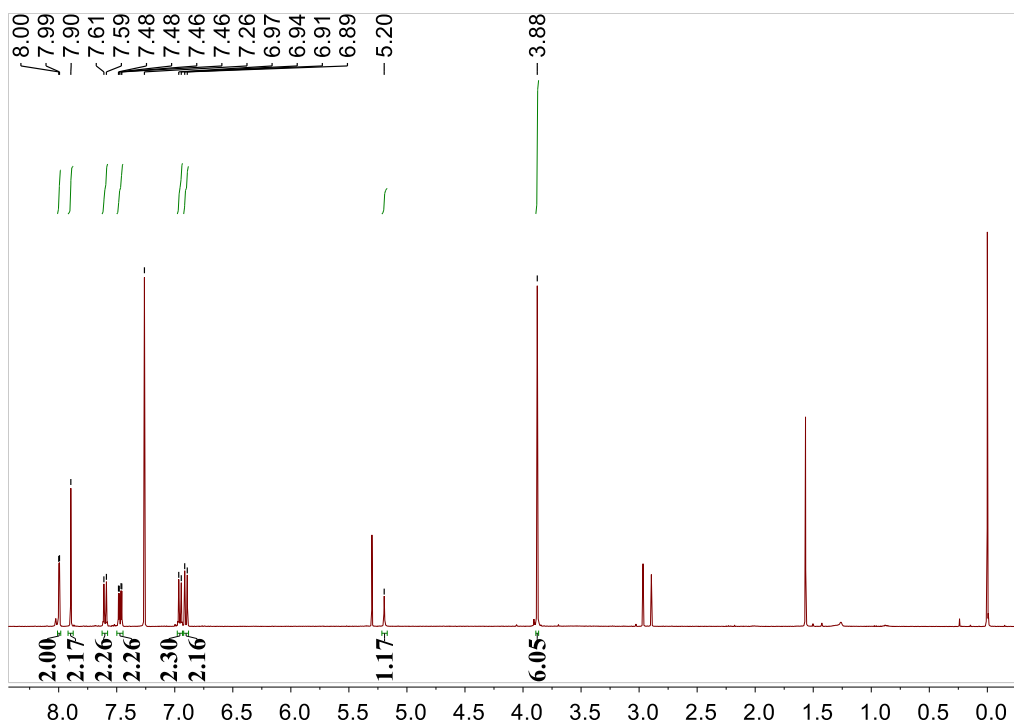
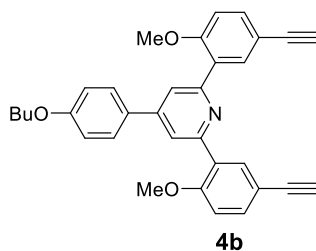


Figure S13. ^1H NMR spectrum (300 MHz, CDCl_3 , 298 K) of **7**.

7.2. Synthesis of **4b**



Compound **7** (1.50 g, 2.50 mmol), $\text{Pd}(\text{PPh}_3)_4$ (175 mg, 0.25 mmol) and CuI (19.0 mg, 0.10 mmol) in 100 mL of TEA were stirred under nitrogen atmosphere. Trimethylsilylacetylene (1.97 g, 20.0 mmol) was added dropwise to the reaction mixture. After stirring at 85 °C for 36 hours, the reaction mixture was evaporated to remove the solvent, and the residue was dissolved in MeOH/THF (1:1, v/v). Excessive amount of K_2CO_3 (1.44 g, 10.4 mmol) was then added, and the mixture were stirred at room temperature for 2 hours. After the reaction was completed, the solvent was evaporated under reduced pressure, and the residue was extracted with $\text{H}_2\text{O}/\text{CH}_2\text{Cl}_2$. The combined organic extracts were dried over anhydrous Na_2SO_4 and evaporated with a rotary evaporator.

The residue was then dissolved in acetonitrile without the purification process. Excessive amounts of 1-bromobutane and K_2CO_3 were added, and the mixture were stirred under reflux overnight. After the reaction was completed, the solvent was evaporated under reduced pressure, and the residue was extracted with $\text{H}_2\text{O}/\text{CH}_2\text{Cl}_2$. The combined organic extracts

were dried over anhydrous Na_2SO_4 and evaporated with a rotary evaporator. The residue was purified by flash column chromatography (petroleum ether/ CH_2Cl_2 , 1 : 1, v/v as the eluent) to afford compound **4b** as the light yellow solid (550 mg, 45%). ^1H NMR (300 MHz, CDCl_3 , room temperature) δ (ppm): 8.03 (d, $J = 3$ Hz, 2H), 7.88 (s, 2H), 7.65 (d, $J = 9$ Hz, 2H), 7.52 (dd, $J = 6, 3$ Hz, 2H), 6.99 (d, $J = 9$ Hz, 2H), 6.97 (d, $J = 9$ Hz, 2H), 4.03 (t, $J = 6$ Hz, 2H), 3.90 (s, 6H), 3.02 (s, 2H), 1.86–1.76 (m, 2H), 1.54–1.48 (m, 2H), 1.00 (t, $J = 7.4$ Hz, 3H).

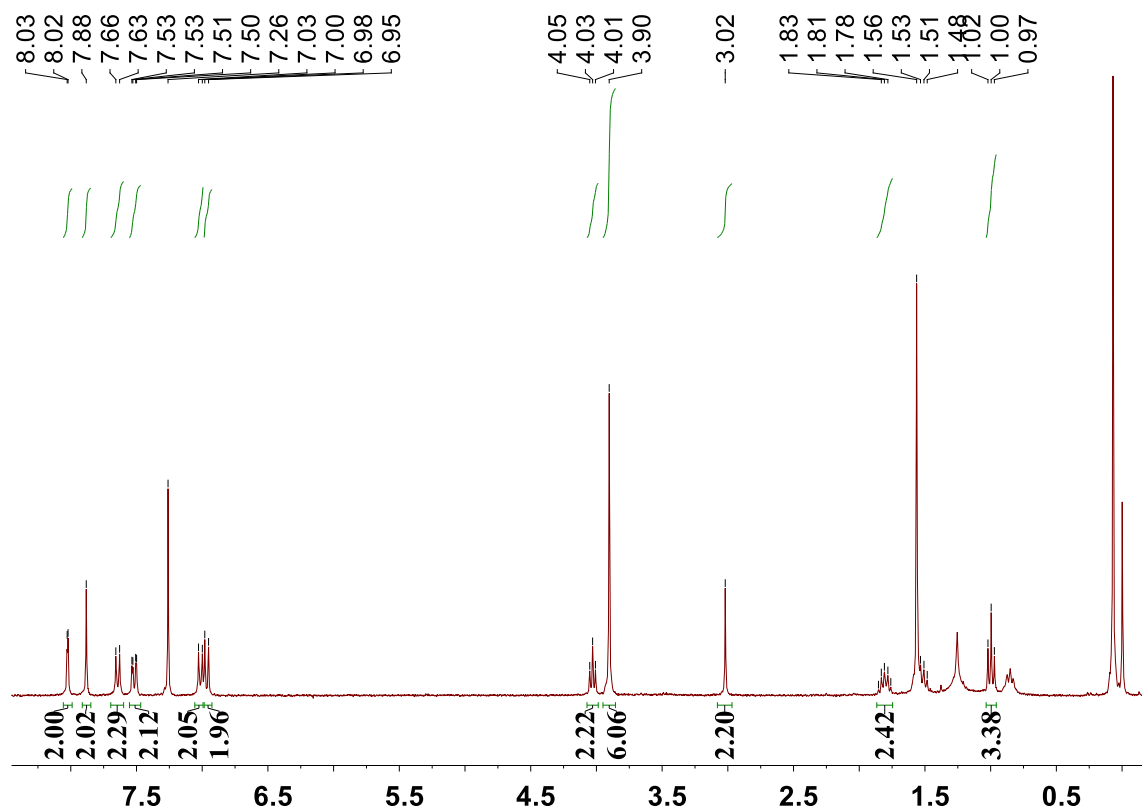
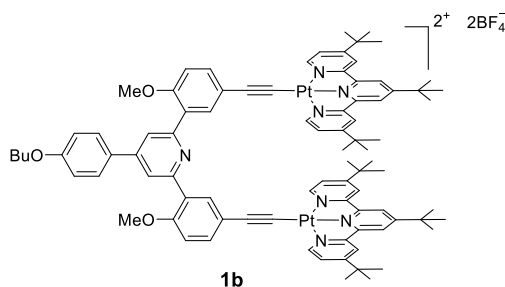


Figure S14. ^1H NMR spectrum (300 MHz, CDCl_3 , room temperature) of **4b**.

7.3. Synthesis of **1b**



Compound **4b** (80 mg, 0.16 mmol), $[\text{Pt}(\text{tpy})\text{Cl}](\text{BF}_4)$ (259 mg, 0.36 mmol), CuI (6 mg, 0.03 mmol) and TEA (5 mL) in CH_2Cl_2 were stirred at room temperature for 48 hours. The mixture was evaporated under reduced pressure, and the residue was purified by flash column chromatograph (neutral alumina, $\text{CH}_2\text{Cl}_2/\text{MeOH}$, 20 : 1 v/v as the eluent) to afford **1b** as a red solid (286 mg, 94%). ^1H NMR (300 MHz, CDCl_3) δ (ppm): 9.01 (d, $J = 5.9$ Hz, 4H), 8.65 (s,

4H), 8.58 (s, 4H), 8.32 (d, $J = 2.3$ Hz, 2H), 8.07 (s, 2H), 7.65 (d, $J = 7.0$ Hz, 2H), 7.54 (d, $J = 7.0$ Hz, 4H), 7.43 (d, $J = 8.4$ Hz, 2H), 6.98 (t, $J = 8.8$ Hz, 4H), 3.99 (t, $J = 6.5$ Hz, 2H), 3.91 (s, 6H), 1.89–1.74 (m, 2H), 1.64–1.46 (m, 36H), 1.31–1.14 (m, 18H), 1.11–1.04 (m, 2H), 0.94 (t, $J = 7.3$ Hz, 3H). ^{13}C NMR (75 MHz, CD_2Cl_2 , room temperature) δ (ppm): 168.4, 167.6, 160.7, 159.2, 156.7, 156.0, 154.4, 154.3, 147.9, 135.2, 133.7, 131.3, 129.9, 128.9, 126.2, 123.6, 121.9, 121.5, 119.8, 115.5, 112.1, 104.2, 96.5, 68.5, 56.4, 37.7, 31.8, 31.1, 30.7, 30.4, 19.8, 14.2. HRMS: m/z : $[\text{M} + \text{H} - 2\text{BF}_4]^{3+}$, 559.2341.

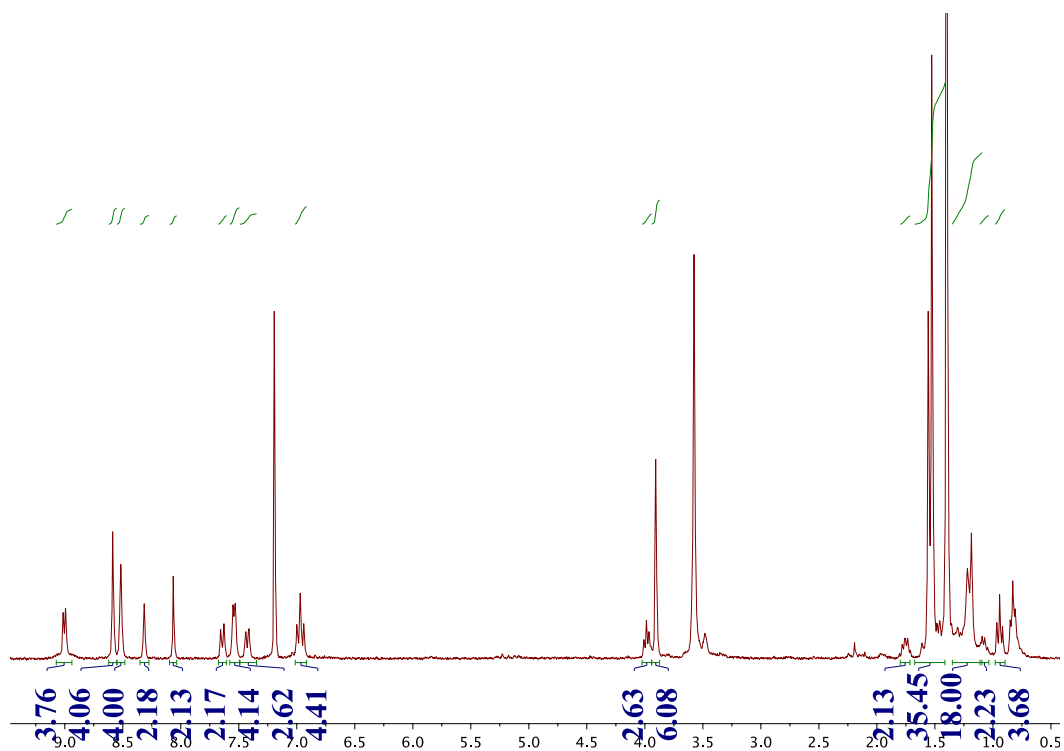


Figure S15. ^1H NMR spectrum (300 MHz, CDCl_3 , room temperature) of **1b**.

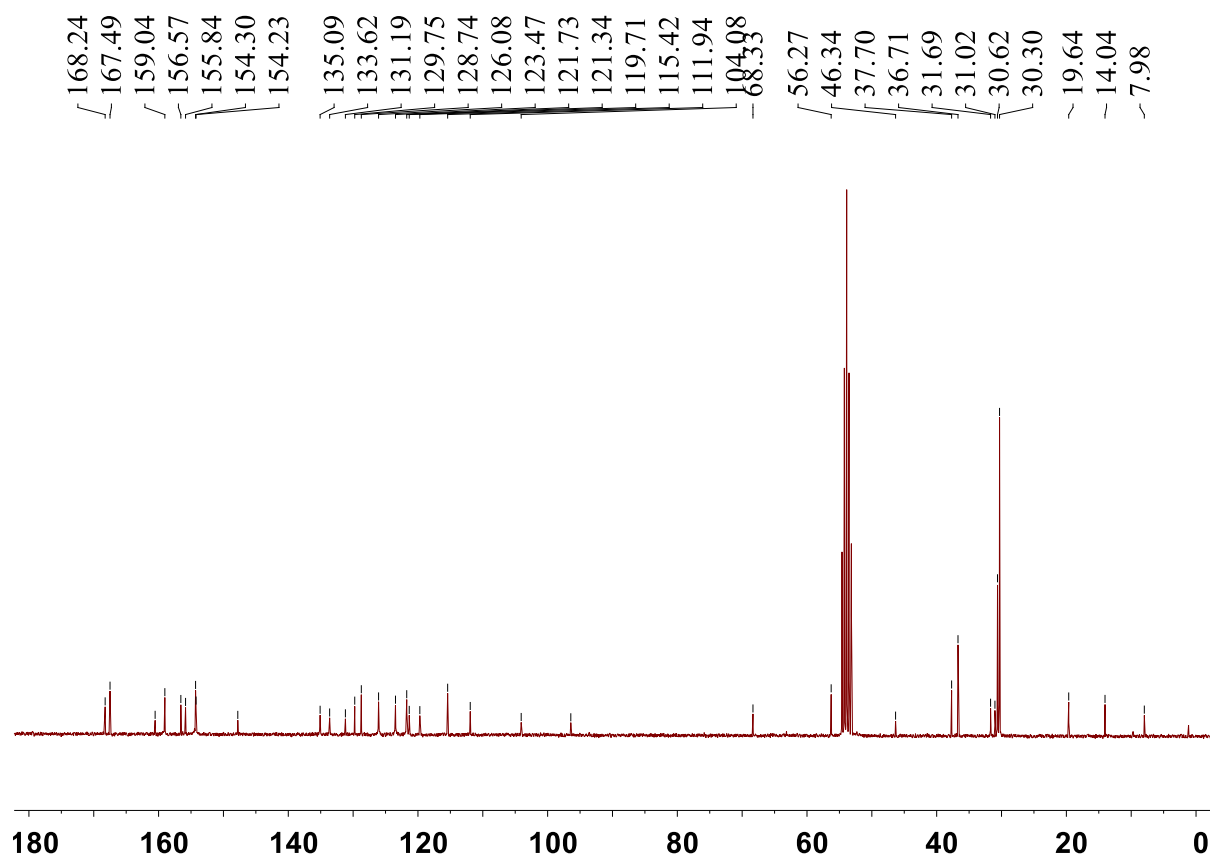


Figure S16. ^{13}C NMR spectrum (75 MHz, CD_2Cl_2 , room temperature) of **1b**.

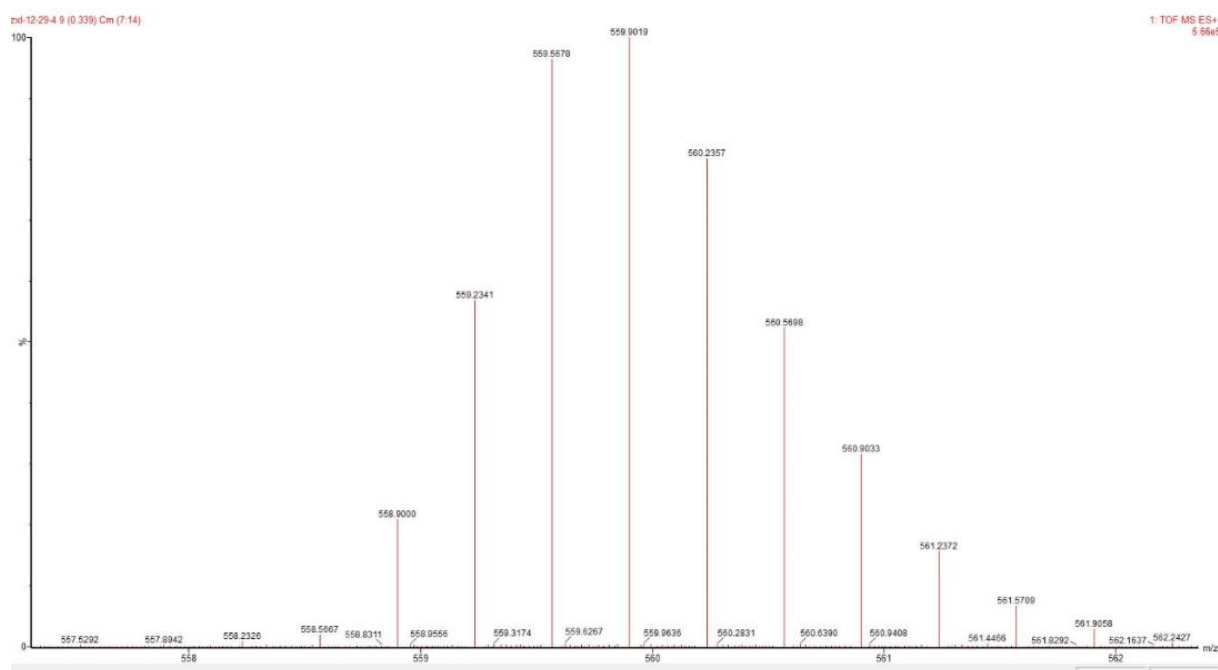
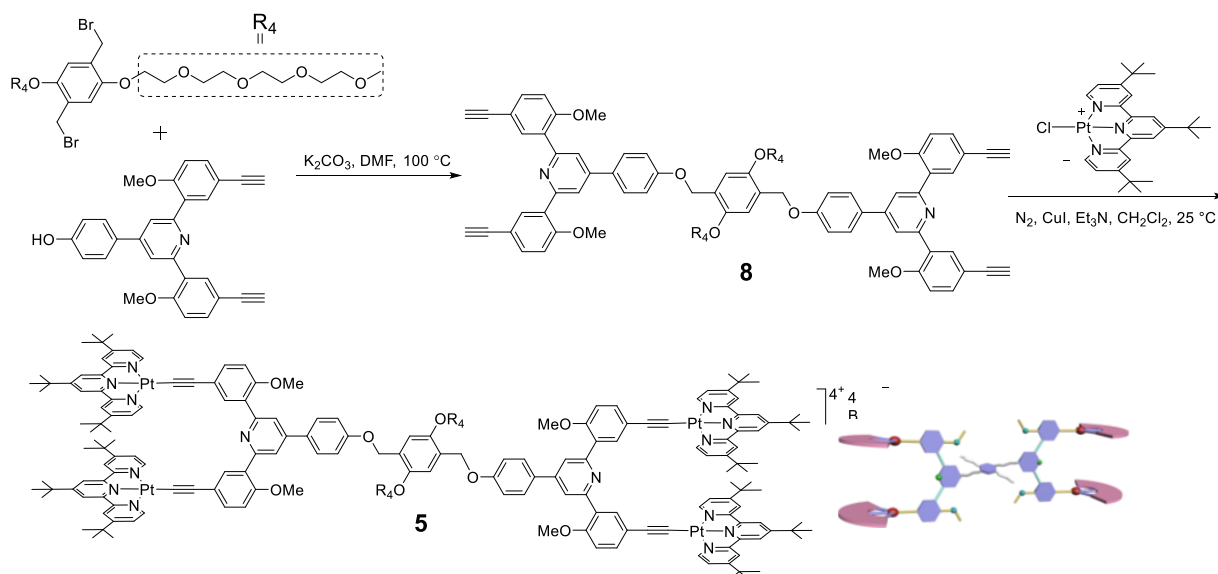
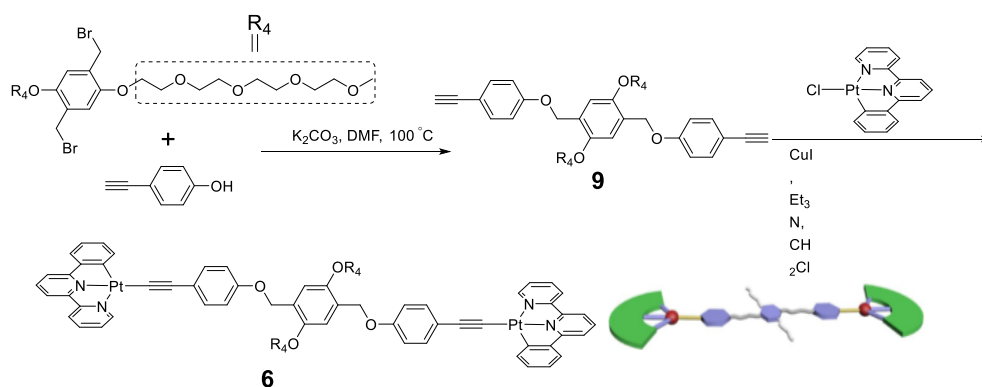


Figure S17. HRMS of **1b**.

8. Synthesis of monomers 5 and 6

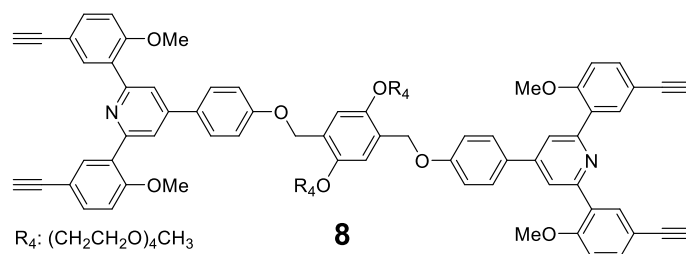


Scheme S2. Synthetic route to monomer **5**.



Scheme S3. Synthetic route to monomer **6**.

8.1 Synthesis of 8



The dibenzylbromide compound (338 mg, 0.50 mmol), dialkynyl compound (539 mg, 1.50 mmol), and K_2CO_3 (345 mg, 2.50 mmol) were mixed together in DMF (25 mL). The resulting mixture was stirred at 100 °C overnight. The solvent was then evaporated under reduced pressure, and the residue was extracted with $\text{H}_2\text{O}/\text{CH}_2\text{Cl}_2$. After the combined organic extracts were dried over anhydrous Na_2SO_4 and evaporated with a rotary evaporator, the residue was

purified by flash column chromatography to afford compound **8** as a white solid (413 mg, 30%). $^1\text{H NMR}$ (300 MHz, CDCl_3) δ (ppm): $^1\text{H NMR}$ (300 MHz, CDCl_3 , room temperature) δ (ppm): 8.03 (d, $J = 3$ Hz, 4H), 7.89 (s, 4H), 7.66 (d, $J = 9$ Hz, 4H), 7.52 (dd, $J = 6, 3$ Hz, 4H), 7.12 (d, $J = 7$ Hz, 4H), 7.08 (s, 2H), 6.97 (d, $J = 9$ Hz, 4H), 5.20 (s, 4H), 4.17 (t, $J = 3$ Hz, 4H), 3.90 (s, 6H), 3.83 (t, $J = 3$ Hz, 4H), 3.69–3.48 (m, 24H), 3.32 (s, 6H), 3.02 (s, 4H).

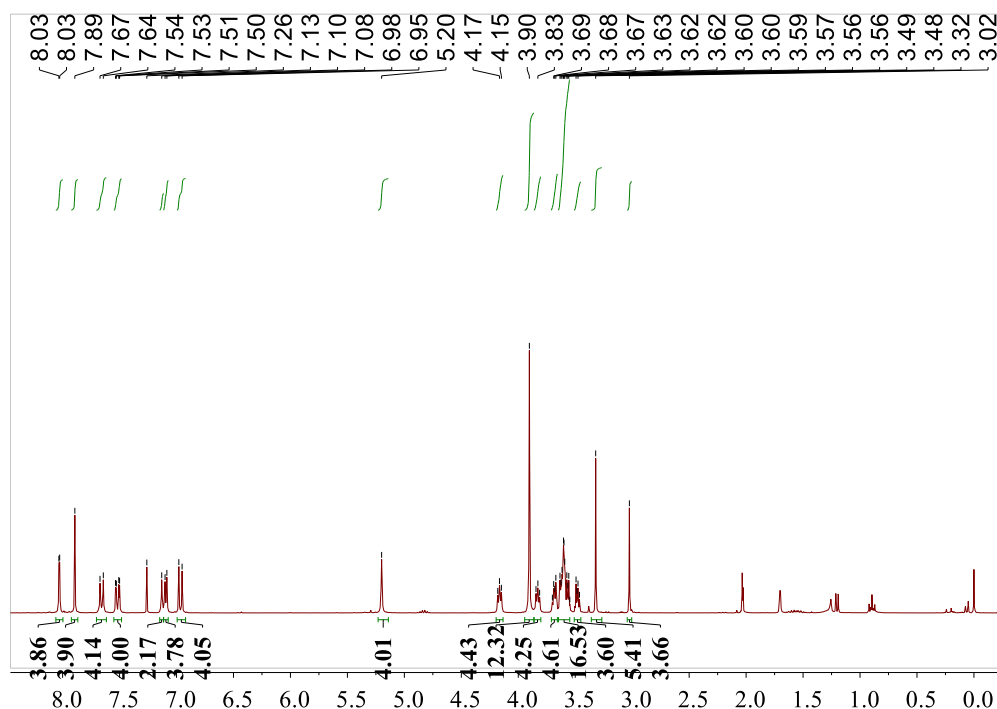
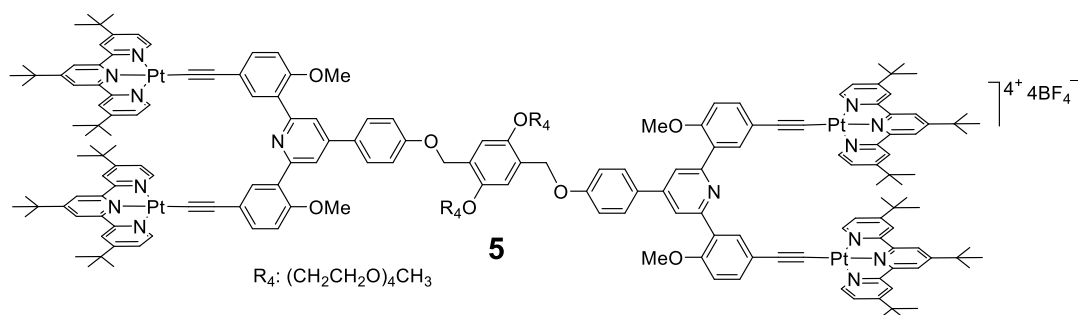


Figure S18. $^1\text{H NMR}$ spectrum (300 MHz, CDCl_3 , 298 K) of **8**.

8.2 Synthesis of **5**



Compound **8** (69 mg, 0.05 mmol), $[\text{Pt}(\text{tpy})\text{Cl}](\text{BF}_4)$ (179 mg, 0.25 mmol), CuI (7.6 mg, 0.04 mmol) and Et_3N (2.5 mL) were dissolved in 20 mL of CH_2Cl_2 and stirred at room temperature for 48 hours. The mixture was evaporated under reduced pressure, and the residue was purified by column chromatography (neutral alumina, $\text{CH}_3\text{OH}/\text{CH}_2\text{Cl}_2$, 100 : 1 v/v as the eluent) to afford **5** as a red solid (252 mg, 76%). $^1\text{H NMR}$ (300 MHz, CDCl_3 , 298 K) δ (ppm): 9.11 (d, $J = 6$ Hz, 8H), 8.68 (s, 8H), 8.60 (s, 8H), 8.11 (d, $J = 2$ Hz, 4H), 7.98 (s, 4H),

7.68 (d, $J = 9$ Hz, 4H), 7.58 (dd, $J = 4, 1$ Hz, 8H), 7.50 (dd, $J = 6, 3$ Hz, 4H), 7.12 (d, $J = 7$ Hz, 4H), 7.08 (s, 2H), 6.97 (d, $J = 9$ Hz, 4H), 5.20 (s, 4H), 4.17 (t, $J = 3$ Hz, 4H), 3.90 (s, 6H), 3.83 (t, $J = 3$ Hz, 4H), 3.69–3.48 (m, 24H), 3.32 (s, 6H). ^{13}C NMR (75 MHz, d_6 -DMSO, room temperature) δ (ppm): 167.1, 166.4, 159.6, 158.2, 156.1, 154.0, 153.4, 152.0, 150.5, 133.4, 132.3, 130.3, 128.3, 127.9, 126.1, 121.2, 118.8, 71.2, 70.0, 69.9, 69.8, 69.7, 69.5, 69.1, 69.0, 62.7, 58.0, 56.2, 52.1, 37.1, 36.1, 30.1, 29.6. HRMS: m/z : $[\text{M} + 2\text{H} - 4\text{BF}_4]^{6+}$, 626.9244.

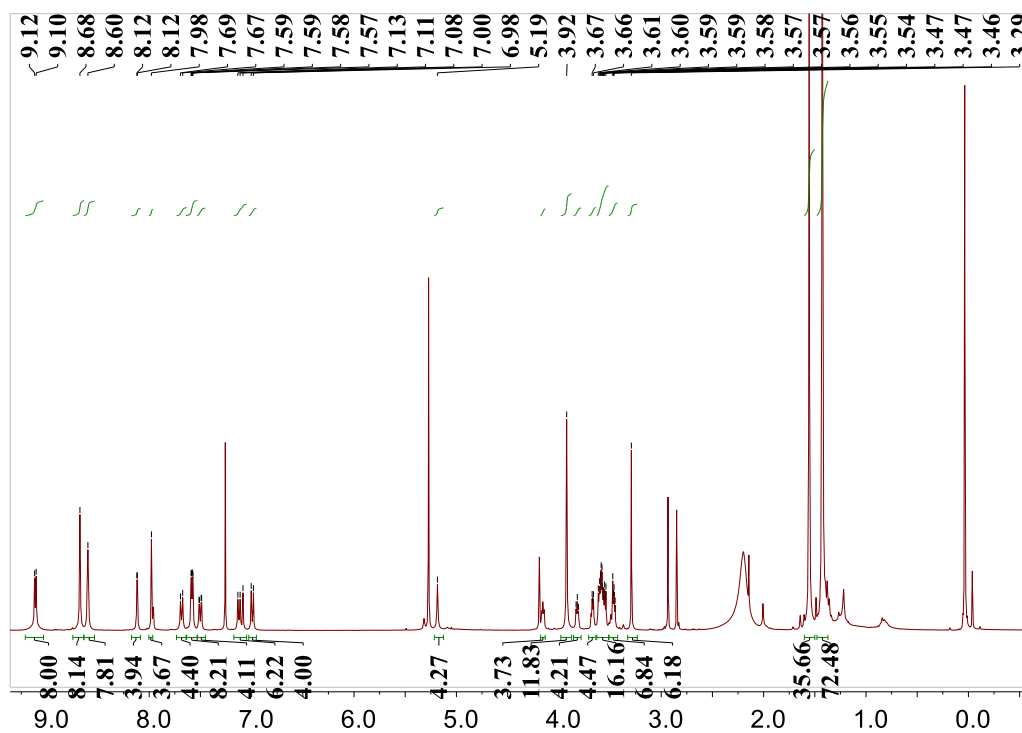


Figure S19. ^1H NMR spectrum (300 MHz, CDCl_3 , 298 K) of **5**.

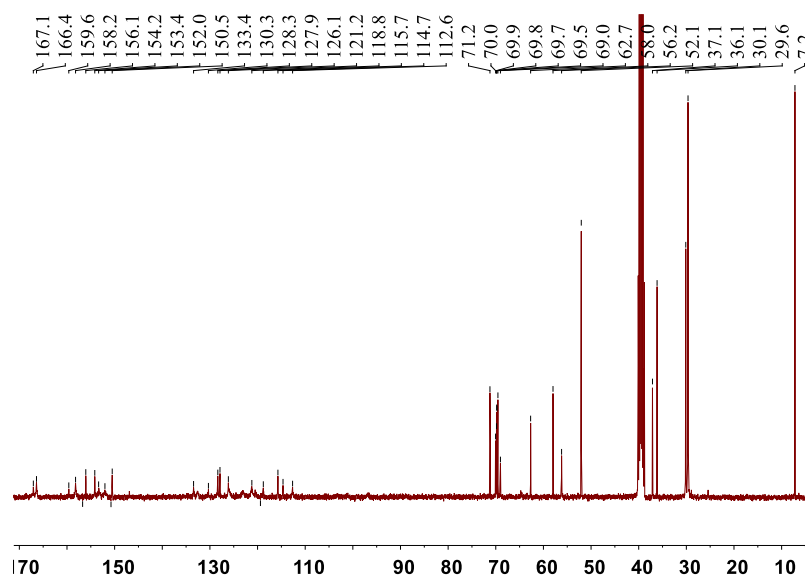


Figure S20. ^{13}C NMR spectrum (75 MHz, d_6 -DMSO, room temperature) of **5**.

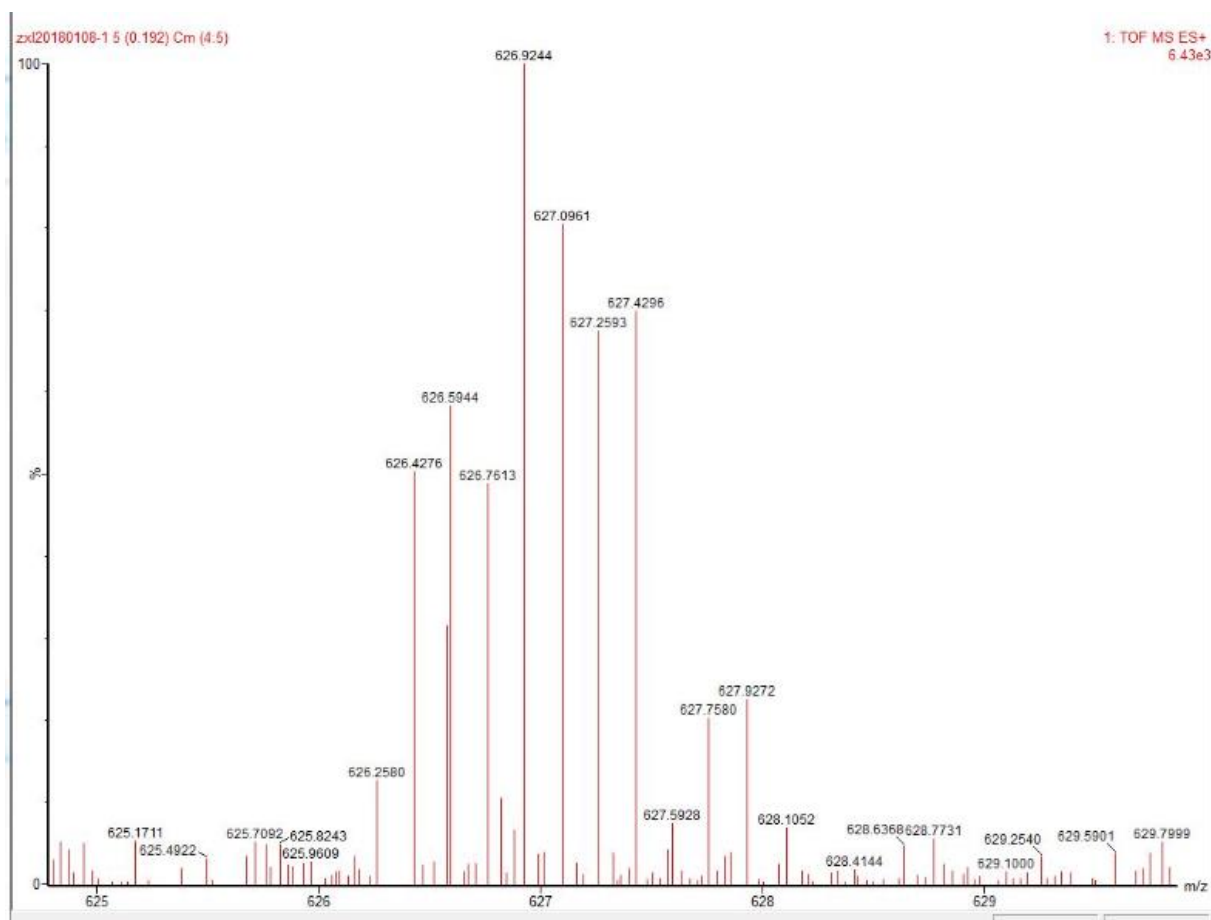
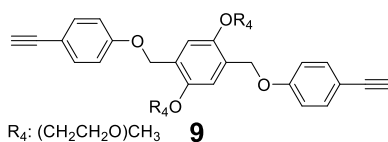


Figure S21. HRMS of **5**.

8.3 Synthesis of **9**



The dibenzylbromide compound (744 mg, 1.10 mmol), 4-hydroxyphenylacetylene (519 mg, 4.40 mmol) and K_2CO_3 (1.10 g, 8.80 mmol) were mixed in DMF (50 mL). The resulting mixture was stirred overnight. The solvent was then evaporated under reduced pressure, and the residue was extracted with $\text{H}_2\text{O}/\text{CH}_2\text{Cl}_2$. After the combined organic extracts were dried over anhydrous Na_2SO_4 and evaporated with a rotary evaporator, the residue was purified by flash column chromatography to afford compound **9** as a light yellow liquid (550 mg, 67%). ^1H NMR (300 MHz, CDCl_3 , 298K) δ (ppm): 7.42 (d, $J = 9$ Hz, 4H), 7.0 (s, 2H), 6.92 (d, $J = 6$ Hz, 4H), 5.12 (s, 4H), 4.11 (t, $J = 3$ Hz, 4H), 3.79 (t, $J = 3$ Hz, 4H), 3.61–3.57 (m, 24H), 3.36 (s, 6H), 2.99 (s, 2H).

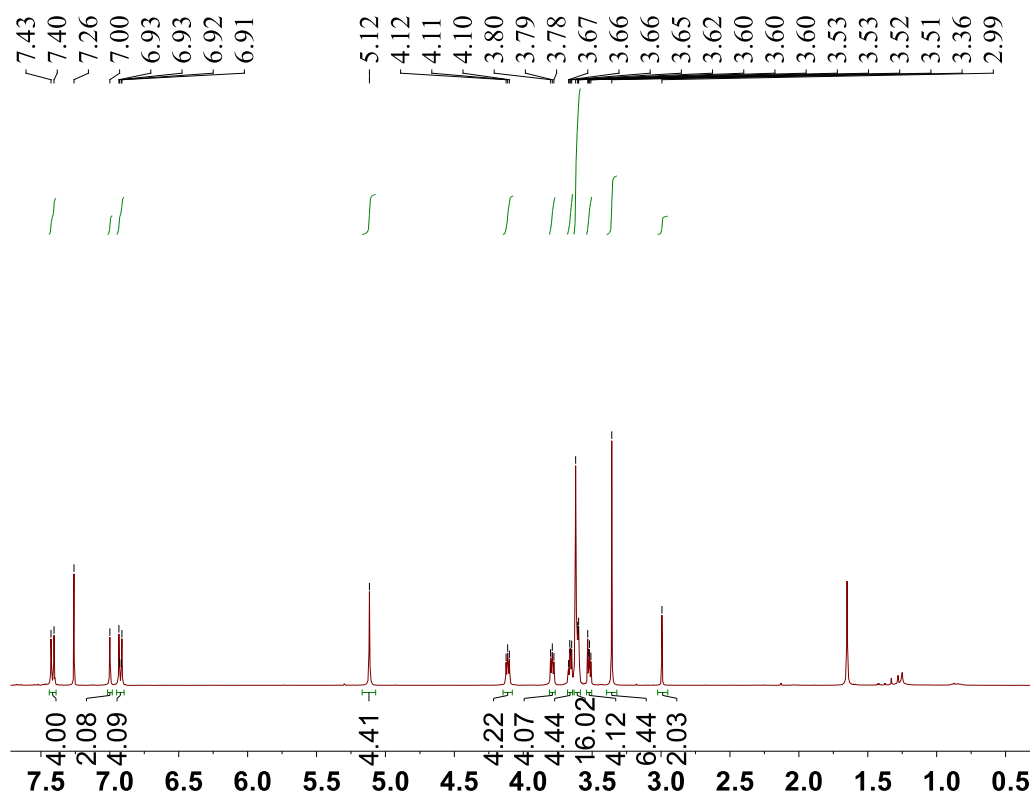
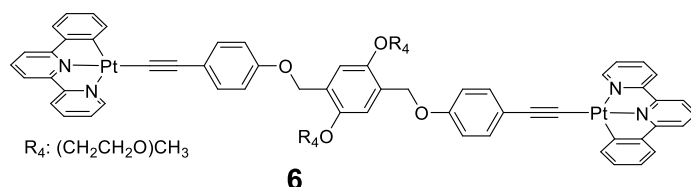


Figure S22. ^1H NMR spectrum (300 MHz, CDCl_3 , 298 K) of **9**.

8.4. Synthesis of **6**



Compound **9** (75 mg, 0.10 mmol), $[\text{Pt}(\text{C}^{\wedge}\text{N}^{\wedge}\text{N})\text{Cl}]$ (106 mg, 0.23 mmol), CuI (4.50 mg, 0.024 mmol) and Et_3N (2.5 mL) were dissolved in 25 mL of CH_2Cl_2 and stirred at room temperature for 48 hours. The mixture was evaporated under reduced pressure, and the residue was purified by column chromatography (neutral alumina, $\text{CH}_3\text{OH}/\text{CH}_2\text{Cl}_2$, 100 : 1 v/v as the eluent) to afford **6** as a dark red solid (60 mg, 37%). ^1H NMR (300 MHz, CDCl_3 , 298 K) δ (ppm): 9.08 (d, $J = 3$ Hz, 2H), 7.93–7.88 (m, 4H), 7.89 (d, $J = 6$ Hz, 2H), 7.69 (t, $J = 6$ Hz, 2H), 7.52–7.41 (m, 10H), 7.28 (d, $J = 6$ Hz, 2H), 7.14 (t, $J = 6$ Hz, 2H), 7.05 (s, 2H), 7.02 (t, $J = 6$ Hz, 2H), 6.90 (d, $J = 6$ Hz, 2H), 5.16 (s, 4H), 4.15 (t, $J = 3$ Hz, 4H), 3.8 (t, $J = 3$ Hz, 4H), 3.66–3.51 (m, 24H), 3.35 (s, 6H), 2.99 (s, 2H). ^{13}C NMR (75 MHz, CDCl_3 , room temperature) δ (ppm): 163.8, 156.8, 155.5, 153.2, 150.0, 149.3, 145.8, 141.7, 137.4, 137.3, 131.8, 130.1, 126.1, 125.3, 123.2, 122.4, 122.0, 120.8, 117.2, 117.1, 113.7, 111.8, 104.4, 102.6, 70.9, 69.8, 69.6, 69.5, 68.8, 67.9, 63.8, 58.0, 53.9, 52.8. HRMS: $[\text{M} + \text{H} + \text{Na}]^{2+}$,

811.4868.

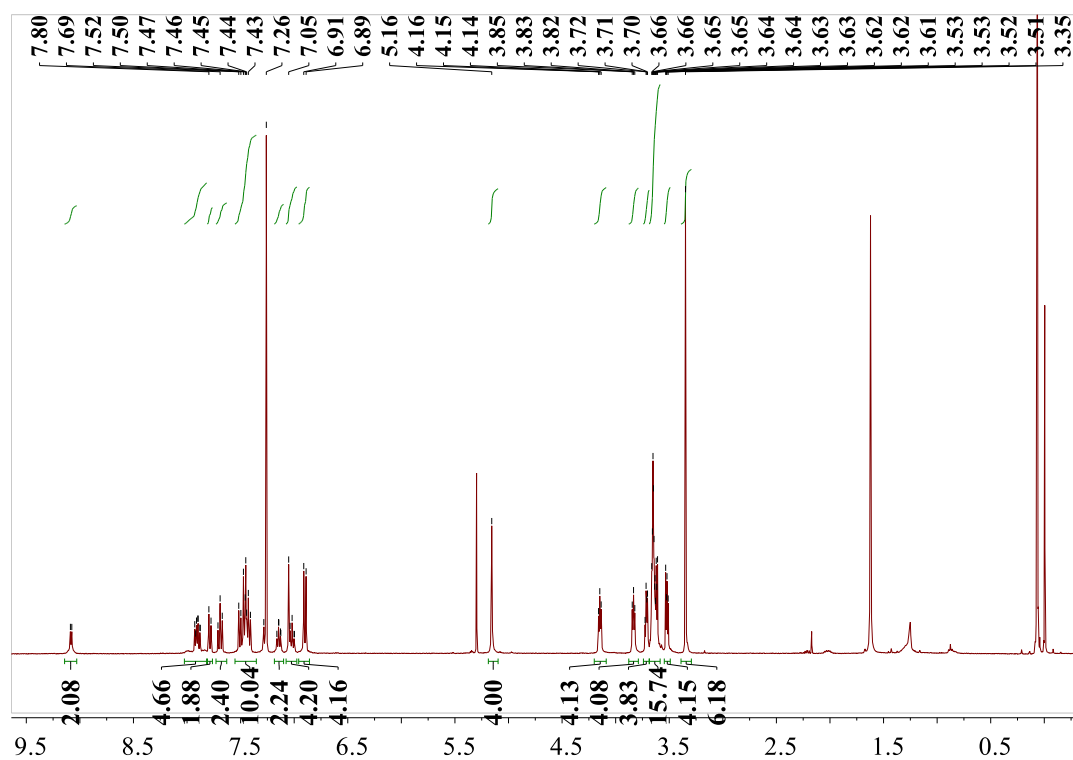


Figure S22. ^1H NMR spectrum (300 MHz, CDCl_3 , 298 K) of **6**.

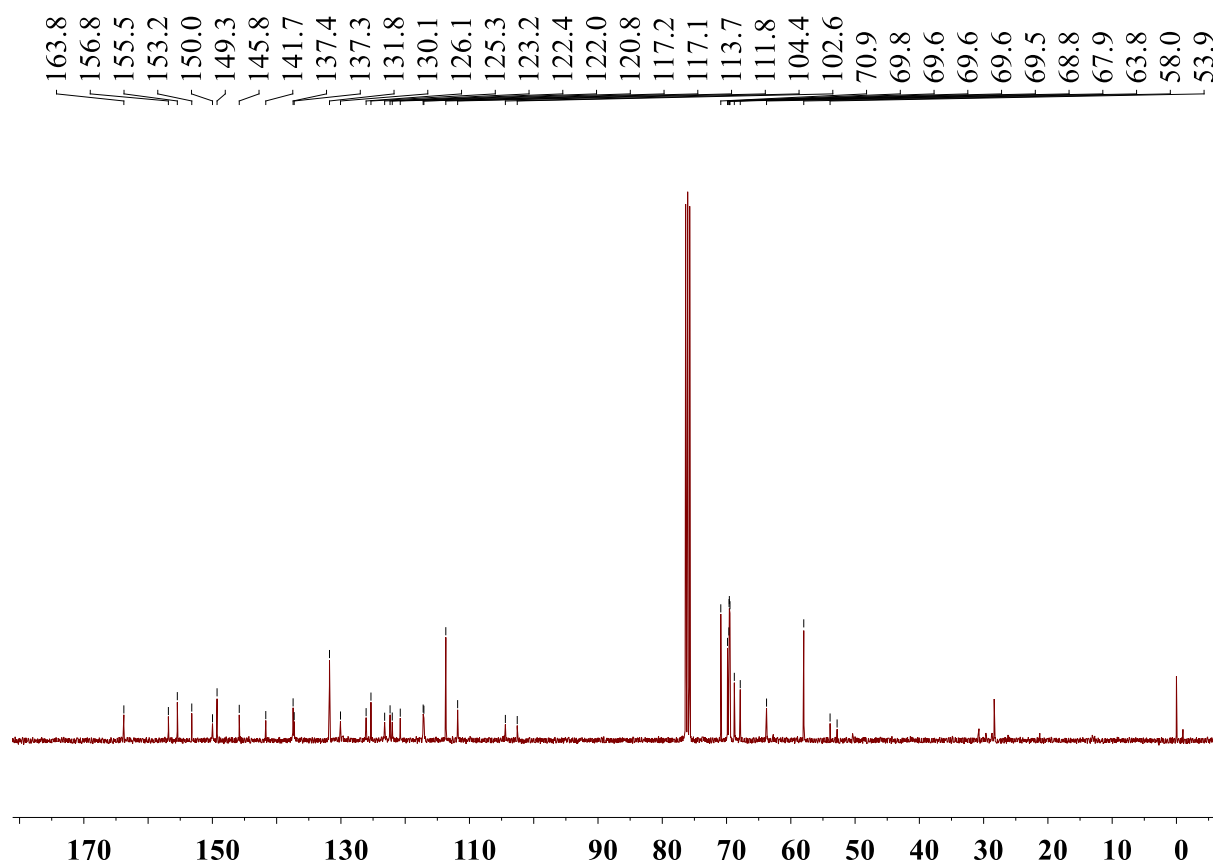


Figure S23. ^{13}C NMR spectrum (75 MHz, CDCl_3 , 298 K) of **6**.

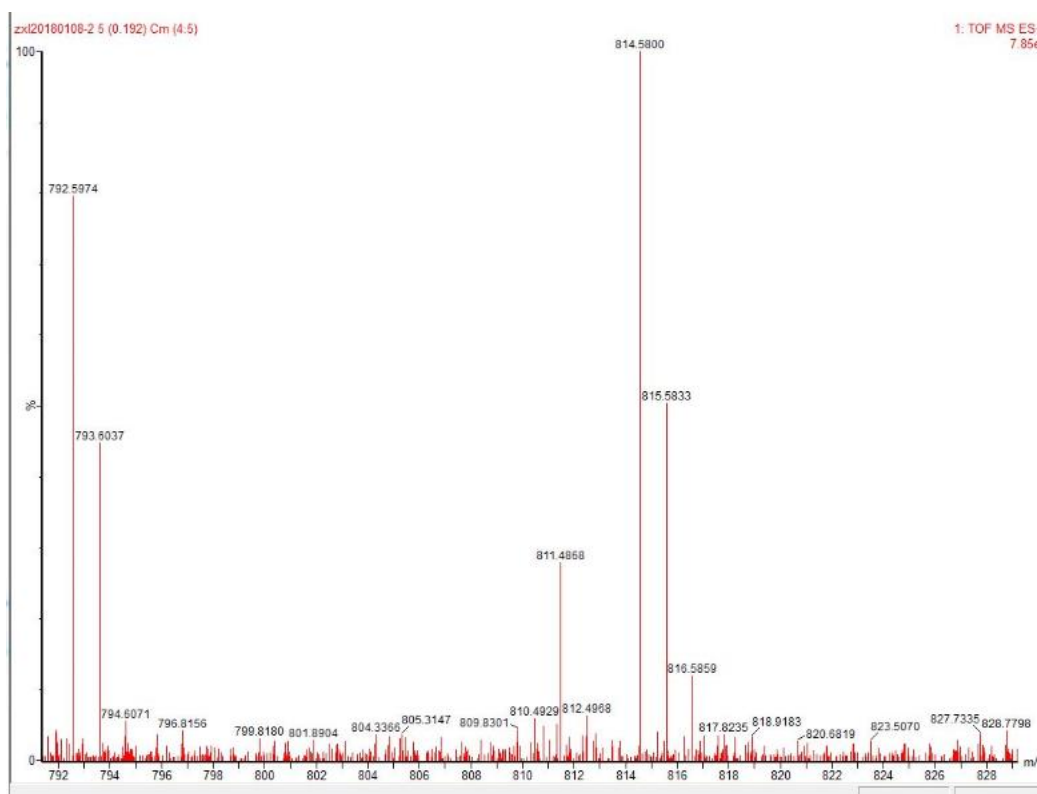


Figure S24. HRMS of **6**.

References:

- [S1] Y. Tanaka, K. M. -C. Wong and V. W. -W. Yam, *Chem. Sci.* 2012, **3**, 1185.
- [S2] Y.-K. Tian, Y.-G. Shi, Z.-S. Yang and F. Wang, *Angew. Chem. Int. Ed.* 2014, **53**, 6090.
- [S3] Z.-J. Li, Y.-F. Han, F. Jin, Z.-C. Gao, Z. Gao, L. Ao and F. Wang, *Dalton Trans.* 2016, **45**, 17290.
- [S4] Z.-J. Li, Y.-F. Han, Z.-C. Gao and F. Wang, *ACS Catal.* 2017, **7**, 4676.
- [S5] W. Lu, B.-X. Mi, M. C.-W. Chan, Z. Hui, C.-M. Che, N. Y. Zhu and S.-T. Lee, *J. Am. Chem. Soc.* 2004, **126**, 495.
- [S6] G. Fabbrini, M. Maggini, and M. Meneghetti, *Phys. Chem. Chem. Phys.* 2007, **9**, 616.
- [S7] Gaussian 09, Revision D.01, M. J. Frisch, G. W. Trucks, H. B. Schlegel, G. E. Scuseria, M. A. Robb, J. R. Cheeseman, G. Scalmani, V. Barone, B. Mennucci, G. A. Petersson, H. Nakatsuji, M. Caricato, X. Li, H. P. Hratchian, A. F. Izmaylov, J. Bloino, G. Zheng, J. L. Sonnenberg, M. Hada, M. Ehara, K. Toyota, R. Fukuda, J. Hasegawa, M. Ishida, T. Nakajima, Y. Honda, O. Kitao, H. Nakai, T. Vreven, J. A. Montgomery, Jr., J. E. Peralta, F. Ogliaro, M. Bearpark, J. J. Heyd, E. Brothers, K. N. Kudin, V. N. Staroverov, T. Keith, R. Kobayashi, J. Normand, K. Raghavachari, A. Rendell, J. C. Burant, S. S. Iyengar, J. Tomasi, M. Cossi, N. Rega, J. M. Millam, M. Klene, J. E. Knox, J. B. Cross, V. Bakken, C. Adamo, J. Jaramillo, R. Gomperts, R. E. Stratmann, O. Yazyev, A. J. Austin, R. Cammi, C. Pomelli, J. W. Ochterski, R. L. Martin, K. Morokuma, V. G. Zakrzewski, G. A. Voth, P. Salvador, J. J. Dannenberg, S. Dapprich, A. D. Daniels, O. Farkas, J. B. Foresman, J. V. Ortiz, J. Cioslowski, and D. J. Fox, Gaussian, Inc., Wallingford CT, 2013.